Oxidation of Copper(I) Hexaaza Macrocyclic Dinuclear Complexes

Albert Poater*

Modeling Lab for Nanostructures and Catalysis (MoLNaC), Dipartimento di Chimica, Università degli Studi di Salerno, via Ponte don Melillo, Fisciano (SA) 84084, Italy

Received: May 1, 2009; Revised Manuscript Received: June 17, 2009

DFT calculations give insight into the formation of peroxo intermediates **1**−**8** from a series of Cu(I) complexes bearing N-hexadentated macrocyclic dinucleating ligands, suffering an oxidation by their interaction with molecular oxygen. The discussion is thus based on the side-on peroxo cores, omitting the case of complex **8** for which the most favored structure is the *trans*-peroxo due to para substitution and the steric encumbrance produced by the methylation of the aminic N atoms. The frontier molecular orbital theory explains deeply the O_2 binding to the Cu(I) complexes, giving key relationships between the energy of particular orbitals of the copper complex before the O_2 binding and the corresponding ones for the free O_2. On the other hand, tools such as the energy decomposition analysis and Mayer bond orders reveal the slight differences due to the different types of ligands.

Introduction

Science has revealed that the binding and activation of O_2 through multiple metal centers play an important role in the catalytic cycle of many metalloenzymes.[1] Proteins such as tyrosinase, hemocyanin, and catechol oxidases[2] contain dinuclear copper active sites with suitability to adopt O_2 in their metallic core structures. Despite the fact that most experimental and theoretical efforts have been focused recently toward mono-copper species,[3] the crystal structure determination of tyrosinase[4] in 2006 has renewed the interest in the understanding of biomimetic species of these dicopper complexes.[2d,5] Reaching a deeper insight into the interaction of O_2 with bioinspired dinuclear Cu(I) complexes is one of the key issues,[2g] and a variety of structural motifs for the binding of O_2 have been reported,[6] but most of these dicopper systems display side-on μ-η^2:η^2-peroxo[7] and bis(μ-oxo)[8] isomeric $[Cu_2O_2]^{2+}$ cores when bonding to O_2 that may easily interconvert. Their relative stability is a product of the steric and also electronic properties of the ligands, as well as the polarity and coordinative power of the solvents and counterions.[9]

Moreover, both $[Cu_2O_2]^{2+}$ cores have been proposed to be the active species in the aromatic hydroxylation process, whereas there is still controversy to reach a final conclusion because in most cases the intermediates have not been experimentally characterized.[10]

Low molecular weight biomimetic models have been of great help in understanding the spectroscopic and structural properties of the active site of these proteins.[11] From a reactivity viewpoint model compounds have shown how subtle variations in ligand design strongly affect their reactivity toward oxygen and of the corresponding oxygenate complex toward its intramolecular oxidation or toward the oxidation of an external substrate.[5e,12]

Tyrosinase model systems that selectively produce aromatic hydroxylation products[13] are available; however, mechanistic pathways are scarce, still not fulfilling all the queries about this type of model mimetic of the tyrosinase, however being in crescendo recently.[14] There are important theoretical contributions reporting the oxidation of external substrates and on hydroxylation of the ligand.[2f,15] Starting from the work of Karlin et al., a thorough analysis[16] of the ligand hydroxylation has revealed part of the mechanism[2f,17] and given insight into the reaction pathway mechanism of an intramolecular aliphatic hydroxylation process[18] and also aromatic[19] as well as non-intramolecular aromatic hydroxylation. Overall, two possibilities to achieve the hydroxylation are now on course, describing either a direct O−O cleavage before the insertion of O_2 in the Cu^I_2 species[20] or the formation of the bis(μ-oxo) core from the peroxo entity.[10,21]

SCHEME 1: $[Cu_2O_2]^{2+}$ Core Structures

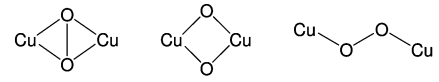

μ-η^2:η^2-peroxo bis–μ–oxo μ-trans-1,2-peroxo

Theoretical analyses based on DFT calculations have shown that the intermediates obtained from the oxidation of the macrocyclic Cu(I) complexes and molecular oxygen generates a variety of side-on Cu_2O_2 motifs.[6d,22] Due to the important role of these intermediates in the tyrosinase action,[2a] here the focus is on a particular description of these intermediates, which might display the shape of Scheme 1. The overall systems studied in this work are displayed in Scheme 2. Those Cu_2O_2 intermediates evolve toward the formation of radically different Cu(II) complexes which depending on the macrocyclic ligand are obtained as a μ-bishydroxo complex,[6d] a μ-hydroxo-μ-phenoxo complex with intramolecular oxidation of the initial ligand,[6d,23] and a terminal bishydroxo complex in para substitution of the phenyl rings,[6d] the latter being the first example of its kind described in the literature.

Previous studies have shown that using different didentate or tridentate alkylamine ligands and depending on the solvent and/or counterions a given Cu(I) complex interacts with molecular oxygen to form both the μ-η^2:η^2-peroxo- or the bis-μ-oxodicopper cores and that these species might be in rapid equilibrium.[12a,24,25] Theoretical calculations revealed that for the systems included in Scheme 2 the side-on peroxo isomer is

* To whom correspondence should be addressed. E-mail: albert.poater@udg.edu.

10.1021/jp9040716 CCC: $40.75
Published on Web 07/14/2009

SCHEME 2: Drawing of the Macrocyclic Ligands of Complexes 1−8

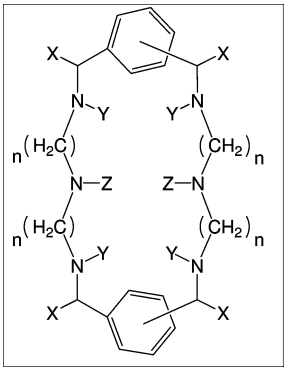

	X	Y	Z	n	Ring substitution
1	-	-	H	2	meta
2	-	-	H	3	meta
3	H	H	H	2	meta
4	H	H	H	3	meta
5	H	CH_3	CH_3	2	meta
6	H	CH_3	CH_3	3	meta
7	H	H	H	2	para
8	H	CH_3	CH_3	2	para

likely to be the only possible isomer since, as indicated previously, no optimized structures for the bis-μ-oxo isomers of **3** and **4** were located.[6d] Overall, there is a lot of controversy about which is the most stable isomer for a system, either the open-shell μ-η^2:η^2-peroxo-Cu^{II}_2 or the closed-shell bis(μ-oxo) complex.[26]

It is envisaged to give insight into the O_2 binding to the Cu(I) complexes through tools such as the Mayer bond orders (MBOs) and the energy decomposition analysis (EDA), especially focusing on the frontier molecular orbital (FMO). The scope of this study is to describe the nature of each complex depending on the slight differences due to the different types of ligands.

Theoretical Background

Energy Decomposition Analysis. The bonding interactions between the molecular fragments A and B in a molecule AB have been analyzed with the energy decomposition scheme of the program package ADF,[27] which is based on the EDA method of Morokuma[28] and the extended-transition-state (ETS) partitioning scheme of Ziegler and Rauk.[29] The bond dissociation energy ΔE between the fragments A and B is partitioned into several contributions which can be identified as physically meaningful quantities. First, ΔE, also called the BE (binding energy) is separated into two major components, ΔE_{def} and ΔE_{int}:

$$\Delta E = \Delta E_{\text{def}} + \Delta E_{\text{int}} \tag{1}$$

ΔE_{def} is the energy which is necessary to promote the fragments A and B from their equilibrium geometry and electronic ground state to the geometry and electronic state which they have in the compound AB. In the case of fragments that do not present a singlet state as the multiplicity ground state, this term must be corrected by an additional term. Therefore, ΔE_{prep} includes a distortion from the geometry of the fragment in its ground state to its geometry in the combined compound as well as an electronic promotion to the state with singlet multiplicity if this is not already the electronic ground-state configuration of the fragment. This additional term to form ΔE_{def} is sometimes called ΔE_{excit}.[30]

ΔE_{int} is the instantaneous interaction energy between the two fragments in the molecule. The latter quantity is the focus of the bonding analysis and can be divided into three main components:

$$\Delta E_{\text{int}} = \Delta E_{\text{elstat}} + \Delta E_{\text{Pauli}} + \Delta E_{\text{orb}} \tag{2}$$

ΔE_{elstat} gives the electrostatic interaction energy between the fragments which is calculated with a frozen electron density distribution in the geometry of the complex. ΔE_{Pauli} gives the repulsive interactions between the fragments which are caused by the fact that two electrons with the same spin cannot occupy the same region in space. The term comprises the four-electron destabilizing interactions between occupied orbitals. ΔE_{Pauli} is calculated by forcing the Kohn−Sham determinant of AB, which results from superimposing fragments A and B, to be orthonormal through antisymmetrization and renormalization. The stabilizing orbital interaction term ΔE_{orb} is calculated in the final step of the analysis when the Kohn−Sham orbitals relax to their final form.

Mayer Bond Order. A definition of bond order due to Wiberg[31] is based on the **P** matrix

$$P_{st} = \sum_{i}^{\text{occupied}} n_i c_{rs} c_{rt} \tag{3}$$

and is applicable to NDO-type theories where the atomic orbital basis forms an orthonormal set. The Wiberg bond order uses the square of the off-diagonal elements of **P**:

$$B_{\text{AB}}^{\text{Wiberg}} = \sum_{s}^{\text{on A}} \sum_{t}^{\text{on B}} P_{st}^{\ 2} \tag{4}$$

Mayer[32] has suggested a method for calculating bond orders from the **P** matrix:

$$B_{\text{AB}}^{\text{Mayer}} = \sum_{s}^{\text{on A}} \sum_{t}^{\text{on B}} (\text{PS})_{st}(\text{PS})_{ts} \tag{5}$$

The Mayer definition can be seen as an extension of the Wiberg index. This leads to the classical integer values for homonuclear diatomics when minimal or small basis sets are used. Noninteger values are found for larger basis sets and in more complicated molecules and these reflect the polarized character of the bonds as well as delocalization and multicenter effects. Mayer bond orders are a valuable tool in the analysis of the bonding in main group[33] and transition metal[34] systems.

Computational Details

The reported calculations were carried out by using the Amsterdam density functional (ADF) package developed by Baerends et al.[35] and vectorized by Ravenek.[36] The numerical integration scheme employed was that of te Velde et al.[37] An uncontracted triple-ζ basis set was used for describing the 3s, 3p, 3d, 4s, and 4p orbitals of copper. For carbon (2s, 2p), nitrogen (2s, 2p), oxygen (2s, 2p), and hydrogen (1s), double-ζ basis sets were employed. All these basis sets were augmented by an extra polarization function.[38] Electrons in lower shells were treated within the frozen core approximation.[35] A set of auxiliary s, p, d, f, and g functions, centered in all nuclei, was introduced to fit the molecular density and Coulomb potential accurately in each SCF cycle.[39] Closed- and open-shell systems were studied within the restricted and unrestricted formalism, respectively. All energetic values were evaluated using a generalized gradient approximation (GGA) that includes a GGA exchange correction of Becke[40] and the GGA correlation correction of Perdew.[41] Several authors have shown that this

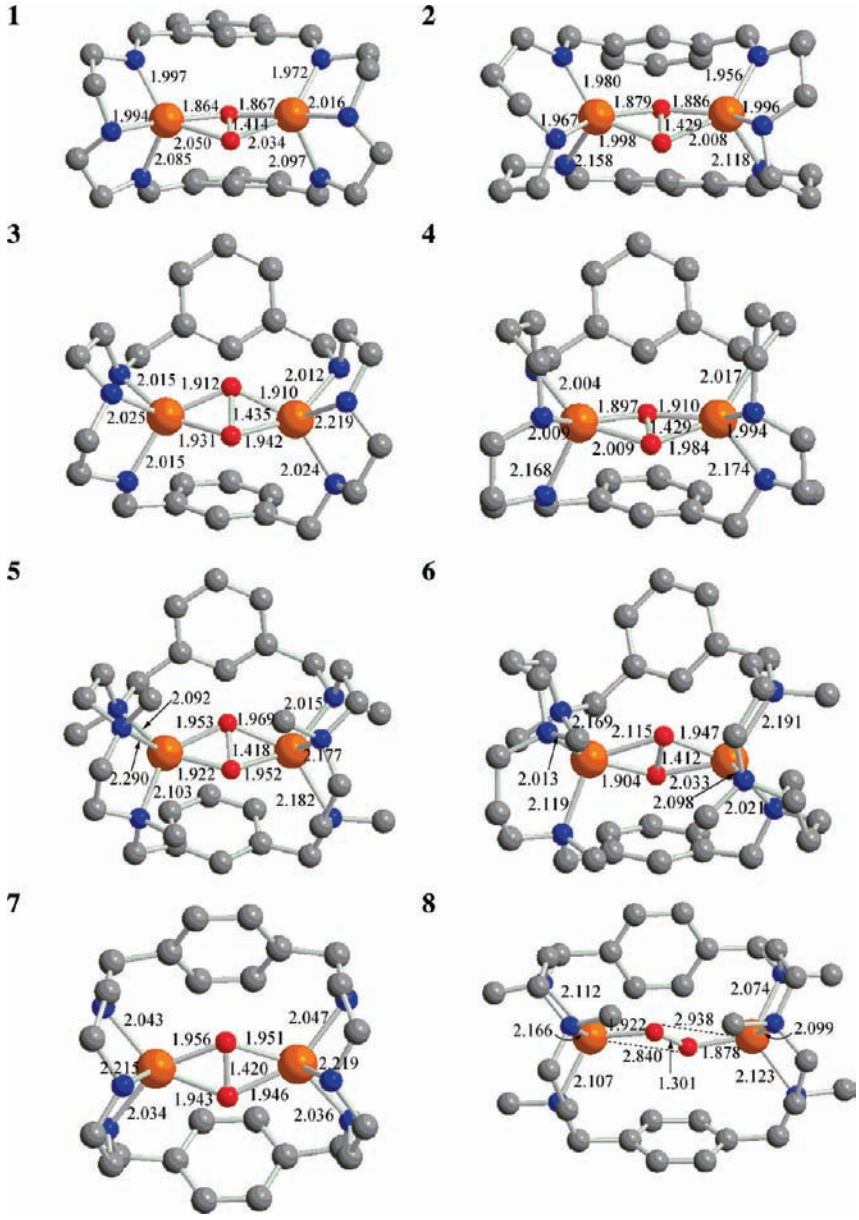

Figure 1. Calculated charged +2 structures for μ-η^2:η^2-peroxo side-on complexes **1**−**7** and *trans*-μ-1,2-peroxo **8**. Hydrogen atoms have been omitted for the sake of clarity.

scheme of calculation provides excellent results for bond dissociation energies.[5d,42] The 2006.01 release of the ADF package was used for all calculations.[43]

Results

The starting point of the study is a series of eight dinuclear copper complexes in Figure 1,[6d] charged +2 closed-shell singlet ground-state structures containing the macrocyclic ligands shown in Scheme 2 and the Cu_2O_2 core. For the reliability of the geometries a validation method similar to that of other studies was used.[44] For the hydroxylated product of system **5** the rms for the bond distances is only 0.067 Å and that for the angles is 1.5°, thus providing confidence in the reliability of the chosen method to reproduce the geometries of the intermediate complexes. The reliability of BP86 relative energies has been substantiated by previous studies.[42,45] Due to the fact that the ligand conformation energy plays an important role in fine-tuning the energetic balance,[46] calculations presented in this work correspond to the full real molecules, without any further modeling. The bis(μ-oxo) species was not located in any case (see Figure 1),[47] in agreement with Cramer[6] for pure exchange-correlation density functionals such as BP86.[48] Futhermore, the equilibrium μ-η^2:η^2-peroxo/bis(μ-oxo) is artificially displaced toward the peroxo species by hybrid functionals such as the B3LYP functional, due to unbalanced correlation corrections, while pure functionals provide better energetics for the relative energy of the peroxo/bis(μ-oxo) isomers.[6,26] Highly correlated ab initio calculations should be used to solve this issue, but unfortunately the large number of atoms in the system precludes this study.

The energy difference between the triplet and the biradical states is low due to the large spatial separation between the two unpaired electrons located on each copper atom, as found in similar copper complexes.[6] Since it has been found for similar species that the triplet state is quite close in energy to the singlet[49] (or even for some particular cases it can be more stable[50]), the relative stability of both states has been checked in all compounds by optimizing the triplet state. In all cases,

TABLE 1: Relative Stability of Singlet and Triplet States for Complexes 1−8

	1	2	3	4	5	6	7	8
ΔE^{S-T}	−7.3	−7.3	−0.7	−0.7	−11.2	−0.1	−1.3	+1.9

TABLE 2: Cu−Cu Distances of 1−8 before and after the O_2 Binding (Å)

	1	2	3	4	5	6	7	8
before	4.165	4.125	5.327	5.579	4.964	4.965	6.172	6.372
after	3.595	3.568	3.455	3.605	3.582	3.738	3.574	4.677

except for **8**, the optimized triplet-state structure presents a higher energy than the optimized singlet-state geometry as is observed in Table 1. In a previous study it was observed that spin-unrestricted broken-symmetry calculations for the singlet diradical state reconverged to the restricted solution.[6d] This means, that, at least at the present BP86 level of theory, the restricted singlet is the ground state. Closed-shell singlet states are favored with respect to open-shell diradical singlet states by DFT.[51] Additionally and related to this effect, it has been shown that the spin density and the DFT orbitals for Cu(II) binuclear complexes are excessively delocalized on the ligands.[52] This overdelocalization is partially corrected when using hybrid functionals, especially those that incorporate a large percentage of exact Hartree−Fock exchange. However, because of the multideterminantal character of the diradical singlet state, sophisticated post-Hartree−Fock calculations are still needed to reach a conclusive answer about the relative stability of closed-shell and open-shell diradical singlet states in the peroxo complexes.[53] Although high-level post-Hartree−Fock methods provide better and more reliable results, they remain prohibitive for molecules containing more than six or seven heavy atoms. In this sense, DFT methods offer a better compromise between the accuracy of the results and the computation time required for large systems such as those analyzed in this work.

Complexes **1**−**7** present a distorted side-on core where the Cu centers adopt a highly distorted square pyramidal geometry, different from the square planar geometry for both copper atoms in complex **8**. This last complex cannot avoid the two characteristics that are against the stability of the side-on core, i.e., the permethylation of the amines and the para substitution

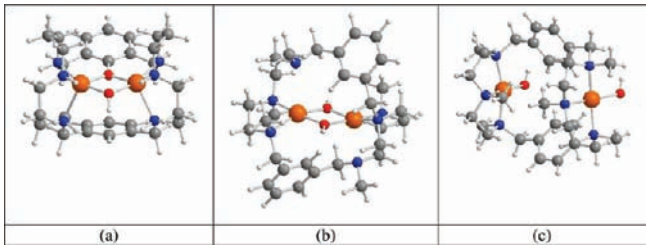

Figure 2. (a) μ-Bishydroxo complex for **4**, (b) μ-hydroxo-μ-phenoxo complex for **5**, and (c) terminal bishydroxo complex for **8**.

TABLE 3: MBOs for Complexes 1−8

	1	2	3	4	5	6	7	8
Cu−Cu	0.195	0.201	0.226	0.213	0.198	0.190	0.209	0.102
O−O	1.071	1.050	1.063	1.036	1.046	1.039	1.068	1.210
Cu−O	0.368	0.339	0.327	0.374	0.369	0.403	0.384	0.532
	0.323	0.358	0.372	0.345	0.395	0.308	0.388	0.188
	0.368	0.347	0.373	0.365	0.357	0.310	0.387	0.194
	0.327	0.365	0.368	0.351	0.382	0.376	0.387	0.554
Cu−O[a]	1.387	1.408	1.440	1.434	1.503	1.397	1.545	1.468

[a] Sum of the four MBO values of the Cu−O interactions.

TABLE 4: Decomposition Energy Analysis for the Cu−μ-η^2:η^2-O_2 Intermediates of Complexes 1−7 (kcal·mol^{-1})

	1	2	3	4	5	6	7
$\Delta E_{def,O_2}$	16.5	18.9	19.8	18.9	17.3	16.3	17.5
$\Delta E_{def,complex}$	12.8	12.7	28.2	28.6	22.4	24.3	42.9
ΔE_{def}	29.3	31.7	48.0	47.6	39.7	40.6	60.4
ΔE_{Pauli}	349.9	369.1	349.6	345.9	356.1	325.8	331.0
ΔE_{elstat}	−198.9	−207.2	−200.8	−198.2	−203.3	−187.8	−194.3
ΔE_{oi}	−226.7	−240.0	−242.6	−235.9	−228.1	−217.0	−226.4
ΔE_{int}	−75.7	−78.1	−93.8	−88.2	−75.3	−79.0	−89.7
ΔE_{excit}	26.8	26.7	26.7	26.7	26.8	26.8	26.8
BE	−19.7	−19.6	−19.1	−13.9	−8.8	−11.6	−2.5

in the aromatic linkers of the corresponding ligand. It is confirmed that, having only one of these handicaps, the molecule reaches the rhombic core, i.e., the $Cu^{II}_2(\mu$-η^2:η^2-$O_2)$ core, but the combination of both evolved to the formation of a *trans*-μ-1,2-end-on core. The permethylation of the amines means an increase of the steric hindrance.

On the other hand, the para substitution of the aromatic rings produces an elongation of the Cu−Cu distance before the O_2 binding. The values from Table 2 confirm these statements. However, this allows the explanation of why complex **8** displays a triplet ground state, with a *trans*-μ-1,2-peroxo core with the copper atoms separated by 4.677 Å (see Figure 1). Furthermore, this multiplicity is explained because of the short distance between oxygen atoms (1.301 Å), similar to that of the free

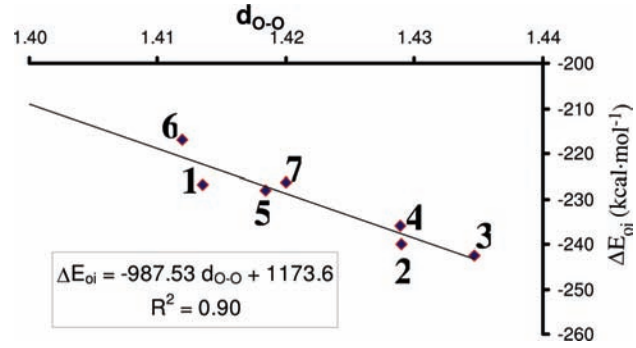

Figure 3. Correlation between the O−O bond length in the μ-η^2:η^2-peroxo intermediates and the orbital interaction energy (ΔE_{oi}).

SCHEME 3: Correlation Diagram Which Describes the Main Orbitals Involved in the Bonding between the Copper Dimer and the Free Molecular Oxygen

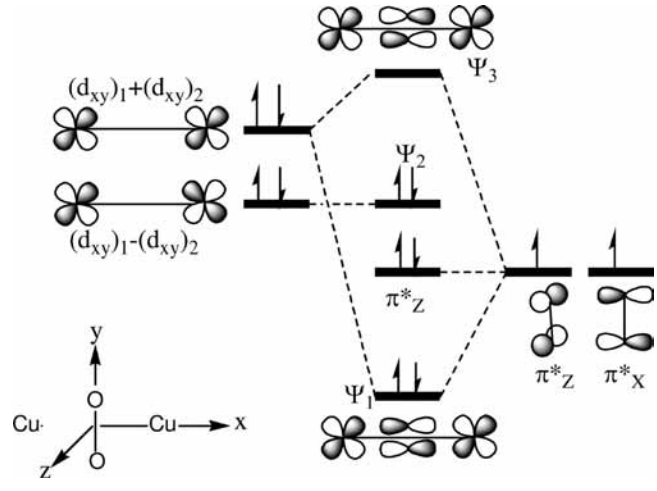

	HOMO	LUMO
1	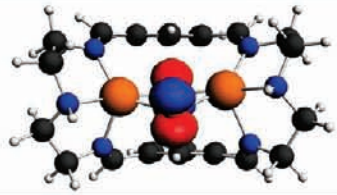	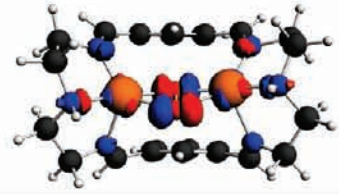
	-236.8	-215.5
2		
	-239.4	-212.5
3		
	-232.0	-211.5
4	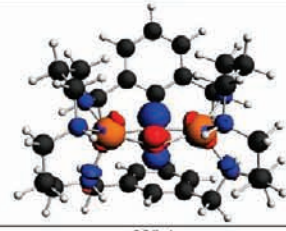	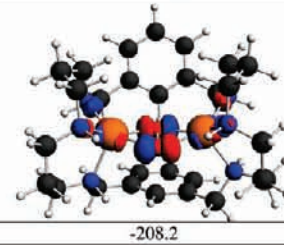
	-230.4	-208.2
5	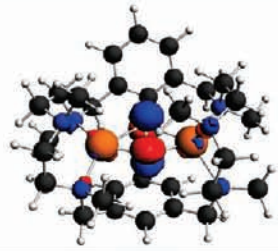	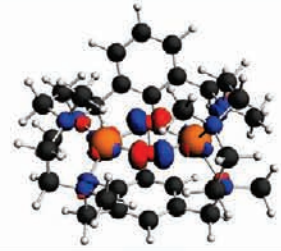
	-231.0	-212.3
6	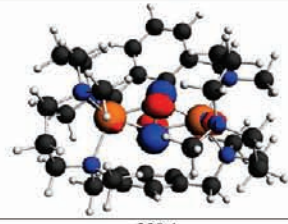	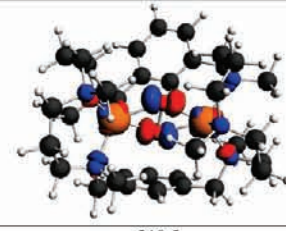
	-230.1	-210.5
7		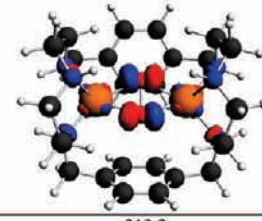
	-232.6	-213.2

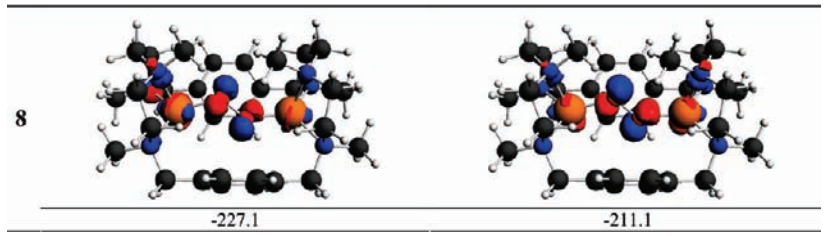

Figure 4. Frontier molecular orbitals of complexes **1**−**8** (energies in kcal·mol^{-1}).

dioxygen molecule (1.218 Å) and much shorter than the O−O bond distances in complexes **1**−**7**. This suggests that complex **8** retains quite a lot of the molecular character of the free O_2, different from what is predicted for similar compounds, but confirmed by stronger structural motives.[54]

The shortening of the Cu···Cu distance with respect to the dinuclear copper(I) complexes before binding to O_2, and the enlargement of the O−O distance with respect to the free molecular oxygen, is a regular behavior for the formation of the side-on peroxo complexes **1**−**7**.

The O_2 binding on these macrocyclic ligands requires more insight because of the different nature of the three types of products obtained from only intermediates **1**−**8**. In Figure 2 the three different optimized products evolved from these eight intermediates are described. Thus, those Cu_2O_2 intermediates evolve toward the formation of radically different Cu(II) complexes which depending on the macrocyclic ligand are obtained as a μ-bishydroxo complex for **4**, a μ-hydroxo-μ-phenoxo complex for **5** with intramolecular oxidation of the initial ligand, and a terminal bishydroxo complex for **8** in the para substitution of the phenyl rings. Complex **4** models the action of the tyrosinase.[6d,19]

To evaluate the strength of the $[Cu_2O_2]^{2+}$ core, an MBO analysis for complexes **1**−**8** listed in Table 3 we envisaged. The MBO values for O−O must be compared with respect to 1.941 of the free O_2 molecule. Immediately a quite constant trend is observed for complexes **1**−**7**, however with lower values than for the free O_2 molecule. Therefore, the O−O bond distance is clearly activated as the MBO decreases when the O_2 is coordinated to both copper atoms. Apart from that, there are different trends that are robust. From complex **1** to **2**, from **3** to **4**, or from **5** to **6** a slight decrease of the MBOs is observed, demonstrating that the addition of a methylenic unit in the alkylic chains that link the amine groups means an increase of the steric hindrance; i.e., it is more difficult for the Cu_2O_2 core to adapt itself inside the central empty space left by the macrocyclic ligand. Furthermore, the permethylation of the amines reveals a decrease of the MBO values, despite complex **6** displaying a higher value than **4**. It is explained from the sum of the Cu−O MBOs that it is quite lower for complex **6** because it displays a quite unsymmetrical core. Complex **6** possesses a unique structure in this family of complexes that allows the explanation of the effect of the permethylation on its side-on peroxo species. If it is compared to complex **4**, the rhombic core suffers a high distortion. Each copper center has two different types of apical coordinating amines, and the relative disposition of the six N atoms is octahedral instead of trigonal prismatic because of this amine permethylation. On the other hand, the odd O−O MBO value for **8** reflects its particular behavior as compared to the other species (vide supra). Furthermore, the Cu−Cu interaction is half with respect to that of the other systems, and the asymmetry of its core reveals two stronger Cu−O bonds and consequently two weaker Cu−O ones.

To gain insight into the nature of the O_2 bonding to form the Cu_2O_2 core, an EDA was carried out. All energetic details about this analysis are collected in Table 4 for complexes **1**−**7** to form the corresponding μ-η^2:η^2-peroxo intermediates. When O_2 binds the binuclear macrocycles, the highest energy released comes from the complexes with Schiff bases as ligands, i.e., species **1** and **2**, the first system displaying the highest value, which explains the fact that the elongation of the linking alkylic chain between imine groups slightly disfavors the O_2 binding. This is reinforced by comparing system **3** with system **4**, but with amines. For the Schiff base systems the difference is smaller due to the rigidity given by the imine groups. Thus, overall, enlarging this chain, the formation of the μ-η^2:η^2-peroxo intermediate is less favored. Then complex **6** is expected to have a lower binding energy than **5**, but really it does not present a perfect rhombic core (vide supra). Anyway, the permethylation of the amine groups in both systems supposes a considerable decrease of the binding energy. Finally, when the effects of the meta and para substitutions of the aromatic ring are compared, i.e., systems **3** and **7**, a sharp decrease of the binding energy is observed due to the long Cu−Cu distance before the insertion of the free O_2 molecule, 6.172 Å for **7** with respect to 5.327 Å for **3**.

The EDA study of the binding energy between the ground state of molecular O_2 and the binuclear macrocycle to form the μ-η^2:η^2-peroxo compounds allows a detailed scheme collected in Table 4 which first decomposes the binding energy into the deformation energy and interaction energy. The deformation energy (ΔE_{def}) is the energy needed to modify the geometry of the ground-state free fragments to attain the geometry that they have in the intermediate. It can be divided into the deformation energy of the dinuclear complex ($\Delta E_{def,complex}$) and the deformation energy of the oxygen molecule ($\Delta E_{def,O_2}$). On the other hand, the interaction energy (ΔE_{int}) is the energy released when the two free deformed fragments in their ground states, i.e., the free O_2 molecule and the macrocyclic ligand bonded to two Cu(I) ions, are brought to the position that they have in the μ-η^2:η^2-peroxo intermediate. This interaction energy may be divided into three parts as seen in eq 2.

The ΔE_{def} total values range from 29.3 kcal·mol^{-1} (**1**) to 60.4 kcal·mol^{-1} (**7**). First, it is necessary to point out that the deformation energy of the O_2 molecule is almost constant for all complexes, ranging from 16.3 kcal·mol^{-1} for complex **6**, which is supposed to display a nonperfect peroxo core, to 19.8 kcal·mol^{-1} for complex **3** (19.8 kcal·mol^{-1}), which is the complex with the most activated O−O bond, i.e., with the largest O−O bond length (1.435 Å). Thus, the differences in deformation energy must be found in the other term corresponding to the ΔE_{def} of the nonoxygenated part of the complexes, ranging from 12.7 to 42.4 kcal·mol^{-1}. It is extremely low for complexes **1** and **2**, bearing Schiff base ligands in their structures that bring rigidity to display by far the shortest Cu−Cu distances before the O_2 binding (see Table 2). The permethylated species **5** and **6** display lower values with respect to the homologous non-

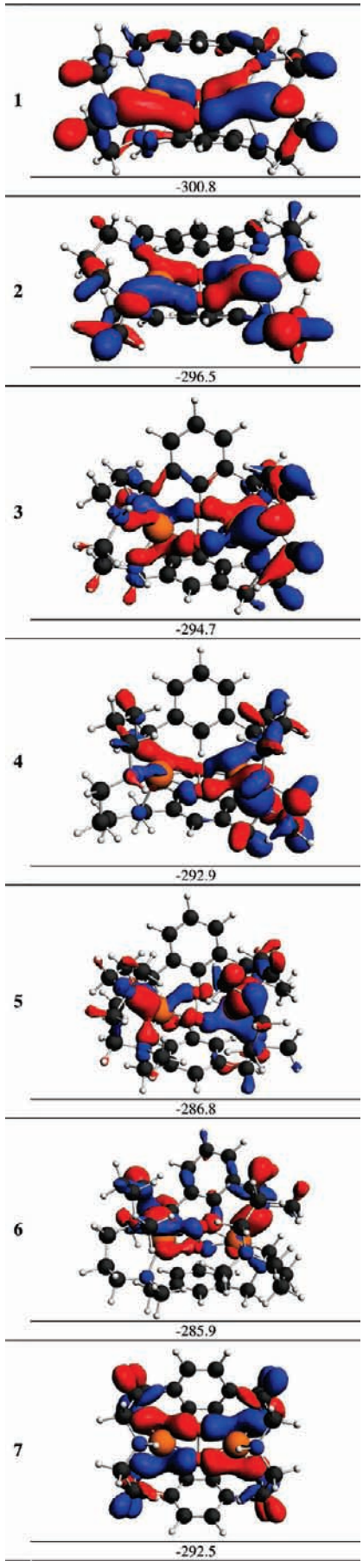

Figure 5. Ψ_1 orbital of complexes **1**−**7**, output of the $(d_{xy})_1 + (d_{xy})_2$ orbital of the dinuclear complex before entering the oxygen molecule with the π^*_x orbital of O_2 (energies in kcal·mol^{-1}).

permethylated ones **3** and **4**, respectively. Thus, the complexes bearing more rigid ligands undergo less deformation in their original structures, leading to lower deformation energies and, in general, more negative binding energies. On the other hand, complex **7** releases an enormous amount of energy (42.4 kcal·mol^{-1}), nearly 50% more than the homologous meta-substituted complex **3**. This fact is thus due to the para substitution of the aromatic rings of the initially dicopper(I) complex that when binding O_2 requires shortening of the Cu···Cu distance from 6.172 to 3.574 Å. Therefore, even though a more rigid ligand favors lower deformation energies, it is necessary to point out that the rigidity must come from the alkylic chains of the ligands, because in the aromatic chains of the ligands the phenyl ring prefers to be substituted in the meta position instead of the para position.

Regarding ΔE_{excit}, due to the triplet → singlet evolution of O_2, nothing must be commented because the differences are lower than 0.1 kcal·mol^{-1}. The ΔE_{int} terms take values from −75.3 kcal·mol^{-1} (**5**) to −89.7 kcal·mol^{-1} (**7**). The rigidity imposed by the Schiff base ligands of complexes **1** and **2** and the permethylation of the amines of complexes **5** and **6** decrease the interaction energy in absolute value. In the latter complexes the Cu_2O_2 core is not placed so nicely as in complexes **3** and **4**. On the other hand, the para substitution of the ring in complex **7** does not strongly decrease this energetic term (from −93.8 kcal·mol^{-1} for complex **3** to −89.7 kcal·mol^{-1} for **7**). This interaction energy term can be further partitioned into the Pauli repulsion energy (ΔE_{Pauli}), the electrostatic interaction (ΔE_{elstat}), and the orbital interaction (ΔE_{oi}) energy terms. There is a correlation with the O−O bond length and the different components of the interaction energy, especially with ΔE_{oi} as can be viewed in Figure 3. Thus, in general and as expected, a larger O−O bond is associated with a larger (in absolute value) ΔE_{oi}. This split of the interaction energy is key to understanding why, for example, the O_2 binding is weaker when all amine groups are permethylated; i.e., there is a sensible decrease of the binding energy from **3** to **5** and from **4** to **6**, according to an even stronger decrease of the covalent interactions included as the ΔE_{oi} term.

To sum up, the higher the basic character of the macrocyclic ligand the lower the binding energy. This is described when going from a complex with a ligand with imine and amine groups to a ligand with only amine groups, i.e., when going from **1** to **3** or from **2** to **4**. Then when going from secondary to tertiary amines, the effect is the same (comparing **3** with **5** and **4** with **6**). Finally the basic character of the ligand is increased when the alkylic chains are increased (comparing **1** with **2** and **3** with **4**). An overview of this explanation can be rationalized from the orbital diagram in Scheme 3, where the interaction between a free oxygen molecule and a dicopper species is displayed. According to Scheme 3, the key interaction is the one involving the $(d_{xy})_1 + (d_{xy})_2$ orbital of the macrocyclic dicopper complex with the π^*_x orbital of the oxygen molecule. When the basicity of the macrocycle increases, the energy of the $(d_{xy})_1 + (d_{xy})_2$ orbital of the copper dimer rises and consequently the energy released in the interaction between the copper dimer and the O_2 molecule decreases.

To check the validity of the simple Scheme 3, first in Figure 4 the energetic values of the highest occupied molecular orbital (ε_H) and the lowest unoccupied molecular orbital (ε_L) of complexes **1**−**8** with their shapes are displayed. It is necessary to point out that despite displaying quite different ligands the shape of the core of the frontier molecular orbitals is nearly the same for complexes **1**−**8**. There is no bonding orbital due to

TABLE 5: Key Orbitals To Gain Insight into the O_2 Binding To Form Complexes 1−7 (kcal·mol^{-1})

Cu−Cu orbital	1	2	3	4	5	6	7
Ψ_1	−300.8	−296.5	−294.7	−292.9	−286.8	−285.9	−292.5
$(d_{xy})_1 + (d_{xy})_2$	−250.2	−252.8	−245.0	−240.6	−243.3	−236.1	−251.0
$[(d_{xy})_1 + (d_{xy})_2] - \Psi_1$	50.6	43.7	49.8	52.3	43.5	49.8	41.5

the π^*_z orbital of the O_2 molecule in the HOMO orbital, supporting the prediction in Scheme 3. Just complex **8** displays a different shape, due to the nonformation of the peroxo intermediate.

Overall, for a better insight I searched for an appropriate orbital corresponding to the d_{xy} orbital of each copper atom, finding it as HOMO − 14 or HOMO − 15 depending on the complex. The significance of the Ψ_1 orbital displayed in Figure 5 for the meta-substituted complexes **1**−**6**, output of the favorable bonding interaction of the dinuclear complexes with O_2, is key to understanding the absolute value of the corresponding binding energies by the relationship BE = 202.9 + $0.745E(\Psi_1)$ with $R^2 = 0.820$. Thus, with a very simple scheme the prediction of the binding energy is feasible, just searching for the energy of just one orbital. In Table 5, the high energetic values of the Ψ_1 orbitals for the permethylated species **5** and **6** explain their lower BEs. This evaluation of the binding energy can be slightly improved by observing the amount of energy corresponding to the overlap of the $(d_{xy})_1 + (d_{xy})_2$ orbital of the nonoxygenated Cu(I) dinuclear complex with the π^*_x orbital of the afterward bonded O_2. Taking into account also the energy of this orbital, the relationship is also quantitative with an agreement of 0.822 for the equation BE = 202.6 + $0.708E(\Psi_1)$ + $0.044E[(d_{xy})_1 + (d_{xy})_2]$. However, the inclusion of this new term is not very significant. On the other hand, instead of including the variable $E[(d_{xy})_1 + (d_{xy})_2]$, the inclusion of a geometrical parameter such as the O−O distance after the O_2 bonding allows an improvement of the agreement of the O_2 bonding ($R^2 = 0.853$) with the equation BE = 324.6 + $0.698E(\Psi_1) - 195.1r_{O-O}$. Especially the behavior of complex **7** does not follow the same trend, influenced surely by its para substitution of the aromatic rings that evidence that the overlap is very low. This suggested that with only the FMO theory and the geometrical parameter r_{O-O} a complete understanding cannot be achieved, this however being possible with a revision of the model, enlarging it with the inclusion of another geometrical parameter. Observing that complex **7** presents the longest Cu−Cu distance before binding O_2, the inclusion of the geometrical parameter that includes the shortenings of the Cu−Cu distance before and after the O_2 binding in the model gave us an excellent agreement for complexes **1**−**7** ($R^2 = 0.953$, BE = −601.5 + $0.573[E[(d_{xy})_1 + (d_{xy})_2] - \Psi_1] - 6.775E[r_{Cu-Cu}$ (before the O_2 binding) − r_{Cu-Cu} (after the O_2 binding)] − $420.3r_{O-O}$). Instead of using the energy of either the Ψ_1 or $(d_{xy})_1$ + $(d_{xy})_2$ orbitals as single variables, I added as a variable the energetic difference between both orbitals. However, this strategy requires further improvement, take for instance including a larger series of systems to increase its statistical validity. Nevertheless, it is feasible to conclude that factors such as the Cu···Cu distance also have an important effect. Indeed, an increase of the Cu···Cu distance in complex **7** after the O_2 binding confirms the stabilization of the $(d_{xy})_1 + (d_{xy})_2$ orbital

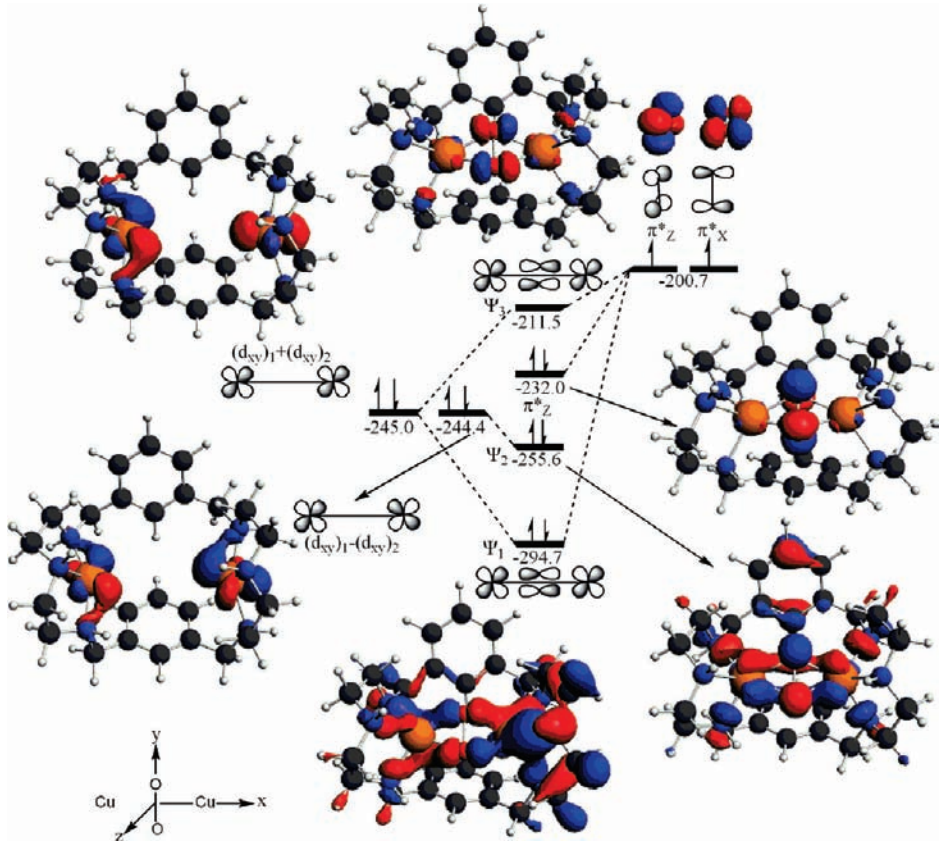

Figure 6. Orbital diagram for the O_2 binding of complex **3** revealing the main interactions between the frontier molecular orbitals and their neighbor orbitals (energies in kcal·mol^{-1}).

of the copper dimer and produces an increase of the absolute value of the binding energy. However, this effect is further compensated by a reduction of the overlap between the $(d_{xy})_1 + (d_{xy})_2$ orbital of the copper dimer and the π^*_x orbital of the O_2 molecule due to the long Cu−Cu distance to overcome; i.e., the low (in absolute value) BE of **7** containing the para-substituted ligand as compared to **3** containing the meta-substituted ligand is related to the larger deformation energy needed to modify the geometry of the dinuclear complex without O_2 to reach the structure that this fragment has in the μ-η^2:η^2-peroxo form.

A schematic diagram of the key orbitals involved in the O_2 binding is displayed in Figure 6, which is a simple mofidication of Scheme 3, however maintaining its nature. It is clear that the supposed nonbonding orbitals had to suffer a slight stabilization because the interactions between orbitals are not pure. Furthermore, the orbitals π^*_z and π^*_x of the free molecular oxygen are higher in energy with respect to the copper ones before interacting. Then the energetic surplus of these degenerated HOMO orbitals of O_2 is strongly stabilized by the dicopper complex. However, the overlap of the $(d_{xy})_1 + (d_{xy})_2$ orbital of the dinuclear complex with the π^*_x orbital of O_2 is confirmed, however finding the Ψ_1 as the HOMO − 14 or 15, depending on the complex.

Conclusions

Theoretical analyses based on DFT calculations have shown that the intermediates obtained from the oxidation of the macrocyclic Cu(I) complexes and molecular oxygen contain a variety of side-on Cu_2O_2 motifs. Those Cu_2O_2 intermediates evolve toward the formation of radically different Cu(II) complexes depending on the macrocyclic ligand.

DFT calculations for dinuclear copper complexes **1**−**8**, containing the macrocyclic ligands shown in Scheme 2 and the $[Cu_2O_2]^{2+}$ core, have proven to be an excellent tool to envisage reactive intermediates that cannot be detected and characterized experimentally. This has allowed rationalization of the nature of the evolved oxidized species based on the nature of the macrocyclic ligand that could not have been understood otherwise. The FMO theory has described thoroughly the binding energies resulting from the O_2 binding, however with a combination with geometrical parameters.

Acknowledgment. I thank the Generalitat de Catalunya for a Beatriu de Pinós postdoctoral fellowship and the INSTM-Italy for a CINECA grant. I also thank X. Ribas, M. Costas, and M. Solà for helpful discussion.

Supporting Information Available: *xyz* coordinates and figures of the calculated **1**−**8** structures and comparison between the X-ray data of complex **5e** and the corresponding geometry. This material is available free of charge via the Internet at http://pubs.acs.org.

References and Notes

(1) (a) Limberg, C. *Angew. Chem., Int. Ed.* **2003**, *42*, 5932–5954. (b) Duran, N.; Esposito, E. *Appl. Catal., B* **2000**, *28*, 83–99. (c) da Silva, G. F. Z.; Tay, W. M.; Ming, L.-J. *J. Biol. Chem.* **2005**, *280*, 16601–16609. (d) Tkatchouk, E.; Fomina, L.; Rumsh, L.; Fomine, S. *Macromolecules* **2003**, *36*, 5607–5612.

(2) (a) Solomon, E. I.; Sundaram, U. M.; Machonkin, T. E. *Chem. Rev.* **1996**, *96*, 2563–2606. (b) Mirica, L. M.; Ottenwaelder, X.; Stack, T. D. P. *Chem. Rev.* **2004**, *104*, 1013–1045. (c) Solomon, E. I.; Chen, P.; Metz, M.; Lee, S.-K.; Palmer, A. E. *Angew. Chem., Int. Ed.* **2001**, *40*, 4570–4590. (d) Karlin, K. D.; Kaderli, S.; Zuberbühler, A. D. *Acc. Chem. Res.* **1997**, *30*, 139–147. (e) Decker, H.; Dillinger, R.; Tuczek, F. *Angew. Chem., Int. Ed.* **2000**, *39*, 1591–1595. (f) Siegbahn, P. E. M. *J. Biol. Inorg. Chem.* **2003**, *8*, 567–576. (g) Lewis, E. A.; Tolman, W. B. *Chem. Rev.* **2004**, *114*, 1047–1076.

(3) (a) Yoshizawa, K.; Kihara, N.; Kamachi, T.; Shiota, Y. *Inorg. Chem.* **2006**, *45*, 3034–3041. (b) Itoh, S.; Taki, M.; Nakao, H.; Holland, P. L.; Tolman, W. B.; Que, L., Jr.; Fukuzumi, S. *Angew. Chem., Int. Ed.* **2000**, *39*, 398–400. (c) Balasubramanian, R.; Rosenzweig, A. C. *Acc. Chem. Res.* **2007**, *40*, 573–580. (d) Rolff, M.; Tuczek, F. *Angew. Chem., Int. Ed.* **2008**, *47*, 2344–2347. (e) Poater, A.; Cavallo, L. *Inorg. Chem.* **2009**, *48*, 2340–2342. (f) K. Yoshizawa, K.; Yt. Shiota, Y. *J. Am. Chem. Soc.* **2006**, *128*, 9873–9881. (g) Yoshizawa, K.; Suzuki, A.; Shiota, Y.; Yamabe, T. *Bull. Chem. Soc. Jpn.* **2000**, *73*, 815–827. (h) Poater, A.; Cavallo, L. *Inorg. Chem.* **2009**, *48*, 4062–4066. (i) de la Lande, A.; Parisel, O.; Gérard, H.; Moliner, V.; Reinaud, O. *Chem.—Eur. J.* **2008**, *14*, 6465–6473. Maiti, D.; Fry, H. C.; Wortink, J. S.; Vance, M. A.; Solomon, E. I.; Karlin, K. D. *J. Am. Chem. Soc.* **2007**, *129*, 264–265. (j) Maiti, D.; Lucas, H. R.; Narducci Sarjeant, A. A.; Karlin, K. D. *J. Am. Chem. Soc.* **2007**, *129*, 6998–6999. (k) Maiti, D.; Lee, D.-H.; Gaoutchenova, K.; Würtele, C.; Holthausen, M. C.; Narducci Sarjeant, A. A.; Sundermeyer, J.; Schindler, S.; Karlin, K. D. *Angew. Chem., Int. Ed.* **2008**, *47*, 82–85. (l) Gherman, B. F.; Tolman, W. B.; Cramer, C. J. *J. Comput. Chem.* **2006**, *27*, 1950–1961.

(4) (a) Matoba, Y.; Kumagai, T.; Yamamoto, A.; Yoshitsu, H.; Sugiyama, M. *J. Biol. Chem.* **2006**, *281*, 8981–8990. (b) Decker, H.; Schweikardt, T.; Tuczek, F. *Angew. Chem., Int. Ed.* **2006**, *45*, 4546–4550.

(5) (a) Karlin, K. D.; Gultneh, Y. *Prog. Inorg. Chem.* **1987**, *35*, 219–327. (b) Sorrell, T. N. *Tetrahedron* **1989**, *45*, 3–68. (c) Karlin, K. D.; Tyeklar, Z. *Adv. Inorg. Biochem.* **1994**, *9*, 123–172. (d) Solomon, E. I.; Lowery, M. D. *Science* **1993**, *259*, 1575–1581. (e) Que Jr, L.; Tolman, W. B. *Angew. Chem., Int. Ed.* **2002**, *41*, 1114–1137. (f) Holland, P. L.; Tolman, W. B. *Coord. Chem. Rev.* **1999**, *192*, 855–869. (g) Würtele, C.; Sander, O.; Lutz, V.; Waitz, T.; Tuczek, F.; Schindler, S. *J. Am. Chem. Soc.* **2009**, *131*, 7544–7545.

(6) (a) Lewin, J. L.; Heppner, D. E.; Cramer, C. J. *J. Biol. Inorg. Chem.* **2007**, *12*, 1221–1234. (b) Cramer, C. J.; Wloch, M.; Piecuch, P.; Puzzarini, C.; Gagliardi, L. *J. Phys. Chem. A* **2006**, *10*, 1991−2004; erratum **2007**, *111*, 4871−4871. (c) Rode, M. F.; Werner, H.-J. *Theor. Chem. Acc.* **2005**, *114*, 309–317. (d) Costas, M.; Ribas, X.; Poater, A.; López-Valbuena, J. M.; Xifra, R.; Company, A.; Duran, M.; Solà, M.; Llobet, A.; Corbella, M.; Usón, M. A.; Mahía, J.; Solans, X.; Shan, X.; Benet-Buchholz, J. *Inorg. Chem.* **2006**, *45*, 3569–3581. (e) Malmqvist, P. A.; Pierloot, K.; Shahi, A. R. M.; Cramer, C. J.; Gagliardi, L. *J. Chem. Phys.* **2008**, *128*, 204109–10. (f) Hong, S.; Huber, S. M.; Gagliardi, L.; Cramer, C. J.; Tolman, W. B. *J. Am. Chem. Soc.* **2007**, *129*, 14190–14192. (g) Cramer, C. J.; Kinal, A.; Wloch, M.; Piecuch, P.; Gagliardi, L. *J. Phys. Chem. A* **2006**, *110*, 11557–11568. (h) Bernardi, F.; Bottoni, A.; Casadio, R.; Fariselli, P.; Rigo, A. *Inorg. Chem.* **1996**, *35*, 5207–5212.

(7) (a) Kitajima, N.; Fujisawa, K.; Morooka, Y. *J. Am. Chem. Soc.* **1989**, *111*, 8976–8978. (b) Kitajima, N.; Fujisawa, K.; Fujimoto, C.; Morooka, Y.; Hashimoto, S.; Kitagawa, T.; Torinmi, K.; Tatsumi, K.; Nakamura, A. *J. Am. Chem. Soc.* **1992**, *114*, 1277–1291.

(8) Mahapatra, S.; Halfen, J. A.; Wilinson, E. C.; Pan, G.; Cramer, C. J.; Que, L., Jr.; Tolman, W. B. *J. Am. Chem. Soc.* **1995**, *117*, 8865–8866.

(9) (a) Kodera, M.; Kajita, Y.; Tachi, Y.; Katayama, K.; Kano, K.; Hirota, S.; Fujinami, S.; Suzuki, M. *Angew. Chem., Int. Ed.* **2004**, *43*, 334–337. (b) Funahashi, Y.; Nishikawa, T.; Wasada-Tsutsui, Y.; Kajita, Y.; Yamaguchi, S.; Arii, H.; Ozawa, T.; Jitsukawa, K.; Tosha, T.; Hirota, S.; Kitagawa, T.; Masuda, H. *J. Am. Chem. Soc.* **2008**, *130*, 16444–16445. (c) Halfen, J. A.; Mahapatra, S.; Wilkinson, E. C.; Kaderli, S.; Young, Jr, V. G.; Que, L., Jr.; Zuberbühler, A. D.; Tolman, W. B. *Science* **1996**, *271*, 1397–1400. (d) Mahapatra, S.; Halfen, J. A.; Tolman, W. B. *J. Am. Chem. Soc.* **1996**, *118*, 11575–11586. (e) Osako, T.; Tachi, Y.; Taki, M.; Fukuzumi, S.; Itoh, S. *Inorg. Chem.* **2001**, *40*, 6604–6609. Hatcher, L. Q.; Vance, M. A.; Narducci Sarjeant, A. A.; Solomon, E. I.; Karlin, K. D. *Inorg. Chem.* **2006**, *45*, 3004–3013. (f) Ottenwaelder, X.; Rudd, D. J.; Corbett, M. C.; Hodgson, K. O.; Hedman, B.; Stack, T. D. P. *J. Am. Chem. Soc.* **2006**, *128*, 9268–9269.

(10) (a) Mirica, L. M.; Vance, M.; Jackson-Rudd, D.; Hedman, B.; Hodgson, K. O.; Solomon, E. I.; Stack, T. D. P. *Science* **2005**, *308*, 1890–1892. (b) Company, A.; Palavicini, S.; Garcia-Bosch, I.; Mas-Ballesté, R.; Que, L., Jr.; Rybak-Akimova, E. V.; Casella, L.; Ribas, X.; Costas, M. *Chem.—Eur. J.* **2008**, *14*, 3535–3538. (c) Funahashi, Y.; Nishikawa, T.; Wasada-Tsutsui, Y.; Kajita, Y.; Yamaguchi, S.; Arii, H.; Ozawa, T.; Jitsukawa, K.; Tosha, T.; Hirota, S.; Kitagawa, T.; Masuda, H. *J. Am. Chem. Soc.* **2008**, *130*, 16444–16445.

(11) (a) Kopf, M.-A.; Karlin, K. D. In *Biomimetic Oxidations Catalyzed by Transition Metal Complexes*; Meunier, B., Ed.; Imperial College Press: London, 2000; pp 309−362. (b) Schindler, S. *Eur. J. Inorg. Chem.* **2000**, 2311–2326.

(12) (a) Tolman, W. B. *Acc. Chem. Res.* **1997**, *30*, 227–237. (b) Mahadevan, V.; DuBois, J. L.; Hedman, B.; Hodgson, K. O.; Stack, T. D. P. *J. Am. Chem. Soc.* **1999**, *121*, 5583–5584. (c) Mahadevan, V.; Henson, M. J.; Solomon, E. I.; Stack, T. D. P. *J. Am. Chem. Soc.* **2000**, *122*, 10249–10250. (d) Taki, M.; Itoh, S.; Fukuzumi, S. *J. Am. Chem. Soc.* **2001**, *123*,

6203–6204. (e) Taki, M.; Teramae, S.; Nagatomo, S.; Tachi, Y.; Kitagawa, T.; Itoh, S.; Fukuzumi, S. *J. Am. Chem. Soc.* **2002**, *124*, 6367–6377. (f) Zhang, C. X.; Liang, H.-C.; Kim, E.-I.; Shearer, J.; Helton, M. E.; Kim, E.; Kaderli, S.; Incarvito, C. D.; Zuberbühler, A. D.; Rheingold, A. L.; Karlin, K. D. *J. Am. Chem. Soc.* **2003**, *125*, 634–635.

(13) (a) Palavicini, S.; Granata, A.; Monzani, E.; Casella, L. *J. Am. Chem. Soc.* **2005**, *127*, 18031–18036. (b) Santagostini, L.; Gullotti, M.; Monzani, E.; Casella, L.; Dillinger, R.; Tuczek, F. *Chem.—Eur. J.* **2000**, *6*, 519–522. (c) Karlin, K. D.; Nasir, M. S.; Cohen, B. I.; Cruse, R. W.; Kaderli, S.; Zuberbühler, A. D. *J. Am. Chem. Soc.* **1994**, *116*, 1324–1336. (d) Mahapatra, S.; Kaderli, S.; Llobet, A.; Neuhold, Y.-M.; Palanche, T.; Halfen, J. A.; Young, V. G., Jr.; Kaden, T. A.; Que, L., Jr.; Zuberbuhler, A. D.; Tolman, W. B. *Inorg. Chem.* **1997**, *36*, 6343–6356. (e) Yamazaki, S.; Itoh, S. *J. Am. Chem. Soc.* **2003**, *125*, 13034–13035. (f) Granata, A.; Monzani, E.; Bubacco, L.; Casella, L. *Chem.—Eur. J.* **2006**, *12*, 2504–2514. (g) Battaini, G.; Monzani, E.; Perotti, A.; Para, C.; Casella, L.; Santagostini, L.; Gullotti, M.; Dillinger, R.; Näther, C.; Tuczek, F. *J. Am. Chem. Soc.* **2003**, *125*, 4185–4198.

(14) Naka, N.; Kondo, Y.; Usui, S.; Hashimoto, Y.; Uchiyama, M. *Adv. Synth. Catal.* **2007**, *349*, 595–600.

(15) (a) Li, L.; Sarjeant, A. N.; Karlin, K. D. *Inorg. Chem.* **2006**, *45*, 7160–7172. (b) Ghosh, D.; Mukherjee, R. *Inorg. Chem.* **1998**, *37*, 6597–6605. (c) Foxon, S. B.; Utz, D.; Astner, J.; Schindler, S.; Thaler, F.; Heinemann, F. W.; Liehr, G.; Mukherjee, J.; Balamurugan, V.; Ghosh, D.; Mukherjee, R. *Dalton Trans.* **2004**, 2321–2328. (d) Siegbahn, P. E. M. *J. Biol. Inorg. Chem.* **2003**, *8*, 577–585. (e) Güell, M.; Siegbahn, P. E. M. *J. Biol. Inorg. Chem.* **2007**, *12*, 1251–1264. (f) Company, A.; Jee, J.-E.; Ribas, X.; López-Valbuena, J. M.; Gómez, L.; Corbella, M.; Llobet, A.; Mahía, J.; Benet-Buchholz, J.; Costas, M.; van Eldik, R. *Inorg. Chem.* **2007**, *46*, 9098–9110. (g) Inoue, T.; Shiota, Y.; Yoshizawa, K. *J. Am. Chem. Soc.* [Online early access]. DOI: 10.1021/ja802618s.

(16) (a) Karlin, K. D.; Dahlstrom, P. L.; Cozzette, S. N.; Scensny, P. M.; Zubieta, J. *J. Chem. Soc., Chem. Commun.* **1981**, 881–882. (b) Karlin, K. D.; Hayes, J. C.; Gultneh, Y.; Cruse, R. W.; McKown, J. W.; Hultchinson, J. P.; Zubieta, J. *J. Am. Chem. Soc.* **1984**, *106*, 2121–2128.

(17) Siegbahn, P. E. M.; Wirstam, M. *J. Am. Chem. Soc.* **2001**, *123*, 11819–11820.

(18) Sander, O.; Henß, A.; Näther, C.; Würtele, C.; Holthausen, M. C.; Schindler, S.; Tuczek, F. *Chem.—Eur. J.* **2008**, *14*, 9714–9729.

(19) Poater, A.; Ribas, X.; Llobet, A.; Cavallo, L.; Solà, M. *J. Am. Chem. Soc.* **2008**, *130*, 17710–17717.

(20) Pidcock, E.; Obias, H. V.; Zhang, C. X.; Karlin, K. D.; Solomon, E. I. *J. Am. Chem. Soc.* **1998**, *120*, 7841–7847.

(21) (a) Mirica, L. M.; Rudd, D. J.; Vance, M. A.; Solomon, E. I.; Hodgson, K. O.; Hedman, B.; Stack, T. D. P. *J. Am. Chem. Soc.* **2006**, *128*, 2654–2665. (b) Holland, P. L.; Rodgers, K. R.; Tolman, W. B. *Angew. Chem., Int. Ed.* **1999**, *38*, 1139–1142.

(22) Lam, B. M. T.; Halfen, J. A.; Young, V. G., Jr.; Hagadorn, J. R.; Holland, P. L.; Lledós, A.; Cucurull-Sánchez, L.; Novoa, J. J.; Álvarez, S.; Tolman, W. B. *Inorg. Chem.* **2000**, *39*, 4059–4072.

(23) (a) Menif, R.; Martell, A. E.; Squattrito, P. J.; Clearfield, A. *Inorg. Chem.* **1990**, *29*, 4723–4729. (b) Becker, M.; Schindler, S.; v. Eldik, R. *Inorg. Chem.* **1994**, *33*, 5370–5371.

(24) (a) Stack, T. D. P. *J. Chem. Soc., Dalton Trans.* **2003**, *10*, 1881–1889. (b) Henson, M. J.; Mukherjee, P.; Root, D. E.; Stack, T. D. P.; Solomon, E. I. *J. Am. Chem. Soc.* **1999**, *121*, 10332–10345.

(25) Liang, H.-C.; Zhang, C. X.; Henson, M. J.; Sommer, R. D.; Hatwell, K. R.; Kaderli, S.; Zuberbühler, A. D.; Rheingold, A. L.; Solomon, E. I.; Karlin, K. D. *J. Am. Chem. Soc.* **2002**, *124*, 4170–4171.

(26) Gherman, B. F.; Cramer, C. J. *Coord. Chem. Rev.* **2008**, *253*, 723–753.

(27) (a) Bickelhaupt, F. M.; Baerends, E. J. In *Reviews in Computational Chemistry*; Lipkowitz, K. B., Boyd, D. B., Eds.; Wiley-VCH: New York, 2000; Vol. 15, p 1. (b) te Velde, G.; Bickelhaupt, F. M.; Baerends, E. J.; van Gisbergen, S. J. A.; Fonseca Guerra, C.; Snijders, J. G.; Ziegler, T. *J. Comput. Chem.* **2001**, *22*, 931–967.

(28) Morokuma, K. *J. Chem. Phys.* **1971**, *55*, 1236–1244. (b) Kitaura, K.; Morokuma, K. *Int. J. Quantum Chem.* **1976**, *10*, 325–340.

(29) Ziegler, T.; Rauk, A. *Theor. Chim. Acta* **1977**, *46*, 1–10.

(30) González-Blanco, O.; Branchadell, V.; Monteyne, K.; Ziegler, T. *Inorg. Chem.* **1998**, *37*, 1744–1748.

(31) Wiberg, K. B. *Tetrahedron* **1968**, *24*, 1083–1096.

(32) (a) Mayer, I. *Chem. Phys. Lett.* **1983**, *97*, 270–277. (b) Mayer, I. *Int. J. Quantum Chem.* **1984**, *26*, 151–154.

(33) (a) Bridgeman, A. J.; Harris, N.; Young, N. A. *Chem. Commun.* **2000**, 1241–1242. (b) Bridgeman, A. J.; Nielsen, N. A. *Inorg. Chim. Acta* **2000**, *303*, 107–115. (c) Bridgeman, A. J.; Rothery, J. *J. Chem. Soc., Dalton Trans.* **1999**, 4077–4082. (d) Bridgeman, A. J.; Rothery, J. *Inorg. Chim. Acta* **1999**, *288*, 17–28. (e) Bridgeman, A. J. *Polyhedron* **1998**, *17*, 2279–2288. (f) Bridgeman, A. J. *J. Chem. Soc., Dalton Trans.* **1997**, 2887–2893. (g) Bridgeman, A. J. *J. Chem. Soc., Dalton Trans.* **1997**, 1323–1329.

(34) (a) Bridgeman, A. J.; Rothery, J. *J. Chem. Soc., Dalton Trans.* **2000**, 211–218. (b) Bridgeman, A. J. *J. Chem. Soc., Dalton Trans.* **1996**, 2601–2607. (c) Bridgeman, A. J. *J. Chem. Soc., Dalton Trans.* **1997**, 4765–4771. (d) Bridgeman, A. J.; Bridgeman, C. H. *Chem. Phys. Lett.* **1997**, *272*, 173–177. (e) Bridgeman, A. J.; Cavigliasso, G.; Ireland, L. R.; Rothery, J. *J. Chem. Soc., Dalton Trans.* **2001**, 2095–2108. (f) Poater, A.; Duran, M.; Jaque, P.; Toro-Labbé, A.; Solà, M. *J. Phys. Chem. B* **2006**, *110*, 6526–6536. (g) Poater, A.; Moradell, S.; Pinilla, E.; Poater, J.; Solà, M.; Martínez, M. A.; Llobet, A. *Dalton Trans.* **2006**, 1188–1196. (h) Poater, A.; Ragone, F.; Correa, A.; Cavallo, L. *J. Am. Chem. Soc.* **2009**, *131*, 9000–9006.

(35) (a) Baerends, E. J.; Ellis, D. E.; Ros, P. *Chem. Phys.* **1973**, *2*, 41–51. (b) Fonseca Guerra, C.; Visser, O.; Snijders, J. G.; te Velde, G.; Baerends, E. J. *Methods and Techniques for Computational Chemistry*; STEF: Cagliari, Italy, 1995. (c) te Velde, G.; Bickelhaupt, F. M.; Baerends, E. J.; Fonseca Guerra, C.; van Gisbergen, S. J. A.; Snijders, J. G.; Ziegler, T. *J. Comput. Chem.* **2001**, *22*, 931–967.

(36) Ravenek, W.; te Riele, H. J. J. In *Algorithms and Applications on Vector and Parallel Computers*; Dekker, T. J., van de Vorst, H. A., Eds.; Elsevier: Amsterdam, 1987.

(37) te Velde, G.; Baerends, E. J. *J. Comput. Phys.* **1992**, *99*, 84–98.

(38) (a) Snijders, J. G.; Baerends, E. J.; Vernooijs, P. *At. Nucl. Data Tables* **1982**, *26*, 483–509. (b) Vernooijs, P.; Snijders, J. G.; Baerends, E. J. *Slater Type Basis Functions for the Whole Periodic System*; Internal Report; Vrije Universiteit Amsterdam: Amsterdam, 1981.

(39) Krijn, J.; Baerends, E. J. *Fit Functions in the HFS Method*; Internal Report (in Dutch); Vrije Universiteit Amsterdam: Amsterdam, 1984.

(40) A, D.; Becke, A. D. *Phys. Rev. A* **1988**, *38*, 3098–3100.

(41) Perdew, J. P. *Phys. Rev. B* **1986**, *33*, 8822–8824.

(42) Li, J.; Schreckenbach, G.; Ziegler, T. *J. Phys. Chem.* **1994**, *98*, 4838–4841. (b) Bickelhaupt, F. M.; Solà, M.; Schleyer, P. v. R. *J. Comput. Chem.* **1995**, *16*, 465–477. (c) Torrent, M.; Deng, L.; Duran, M.; Solà, M.; Ziegler, T. *Organometallics* **1997**, *16*, 13–19. (d) Torrent, M.; Deng, L.; Duran, M.; Solà, M.; Ziegler, T. *Can. J. Chem.* **1999**, *77*, 1476–1491. (e) Deng, L.; Ziegler, T. *Organometallics* **1997**, *16*, 716–724. (f) Deng, L.; Ziegler, T. *Organometallics* **1996**, *15*, 3011–3021.

(43) ADF 2000 and ADF 2007: Baerends, E. J.; Autschbach, J. A.; Bérces, A.; Bickelhaupt, F. M.; Bo, C.; Boerrigter, P. M.; Cavallo, L.; Chong, D. P.; Deng, L.; Dickson, R. M. Ellis, D. E.; van Faassen, M.; Fan, L.; Fischer, T. H.; Fonseca Guerra, C.; van Gisbergen, S. J. A.; Groeneveld, J. A.; Gritsenko, O. V.; Grüning, M.; Harris, F. E.; van den Hoek, P.; Jacob, C. R.; Jacobsen, H.; Jensen, L.; van Kessel, G.; Kootstra, F.; van Lenthe, E.; McCormack, D. A.; Michalak, A.; Neugebauer, J.; Nicu, V. P.; Osinga, V. P.; Patchkovskii, S.; Philipsen, P. H. T.; Post, D.; Pye, C. C.; Ravenek, W.; Ros, P.; Schipper, P. R. T.; Schreckenbach, G.; Snijders, J. G.; Solà, M.; Swart, M.; Swerhone, D.; te Velde, G.; Vernooijs, P.; Versluis, L.; Visscher, L.; Visser, O.; Wang, F.; Wesolowski, T. A.; van Wezenbeek, E. M.; Wiesenekker, G.; Wolff, S. K.; Woo, T. K., Yakovlev, A. L.; Ziegler, T., Vrije Universiteit Amsterdam, The Netherlands, 2007.

(44) (a) Duran, J.; Polo, A.; Real, J.; Benet-Buchholz, J.; Poater, A.; Solà, M. *Eur. J. Inorg. Chem.* **2003**, 4147–4151. (b) Sala, X.; Plantalech, E.; Romero, I.; Rodríguez, M.; Llobet, A.; Poater, A.; Duran, M.; Solà, M.; Jansat, S.; Gómez, M.; Parella, T.; Stoeckli-Evans, H.; Benet-Buchholz, J. *Chem.—Eur. J.* **2006**, *12*, 2798–2807. (c) Poater, A.; Moradell, S.; Pinilla, E.; Poater, J.; Solà, M.; Martínez, M. A.; Llobet, A. *Dalton Trans.* **2006**, 1188–1196. (d) Mola, J.; Romero, I.; Rodríguez, M.; Llobet, A.; Parella, T.; Campelo, J. M.; Luna, D.; Marinas, J. M.; Parella, T.; Poater, A.; Duran, M.; Solà, M. *Inorg. Chem.* **2006**, *45*, 10520–10529.

(45) (a) Martín, N.; Altable, M.; Filippone, S.; Martín-Domenech, A.; Poater, A.; Solà, M. *Chem.—Eur. J.* **2005**, *11*, 2716–2729. (b) Ribas, X.; Xifra, R.; Parella, T.; Poater, A.; Solà, M.; Llobet, A. *Angew. Chem., Int. Ed.* **2006**, *45*, 2941–2944. (c) Xifra, R.; Ribas, X.; Llobet, A.; Poater, A.; Duran, M.; Solà, M.; Stack, T. D. P.; Benet-Buchholz, J.; Donnadieu, B.; Mahía, J.; Parella, T. *Chem.—Eur. J.* **2005**, *11*, 5146–5156.

(46) Bérces, A. *Inorg. Chem.* **1997**, *36*, 4831–4837.

(47) (a) Company, A.; Gómez, L.; Mas-Ballesté, R.; Korendovych, I. V.; Ribas, X.; Poater, A.; Parella, T.; Fontrodona, X.; Benet-Buchholz, J.; Solà, M.; Que, L., Jr.; Rybak-Akimova, E. V.; Costas, M. *Inorg. Chem.* **2007**, *46*, 4997–5012. (b) Company, A.; Gómez, L.; Mas-Ballesté, R.; Korendovych, I. V.; Ribas, X.; Poater, A.; Parella, T.; Fontrodona, X.; Benet-Buchholz, J.; Solà, M.; Que, L., Jr.; Rybak-Akimova, E. V.; Costas, M. *Inorg. Chem.* **2006**, *45*, 5239–5241.

(48) ADF results only support the peroxo species, but these species were recently found with Gaussian,[19] however, to be energetically less stable.

(49) (a) Flock, M.; Pierloot, K. *J. Phys. Chem. A* **1999**, *103*, 95–102. (b) Mahapatra, S.; Halfen, J. A.; Wilkinson, E. C.; Pan, G.; Wang, X.; Young, V. G., Jr.; Cramer, C. J.; Que, L., Jr.; Tolman, W. B. *J. Am. Chem. Soc.* **1996**, *118*, 11555–11574.

(50) Lind, T.; Siegbahn, P. E. M.; Crabtree, R. H. *J. Phys. Chem. B* **1999**, *103*, 1193–1202.

(51) (a) Braïda, B.; Hiberty, P. C.; Savin, A. *J. Phys. Chem. A* **1998**, *102*, 7872–7877. (b) Sodupe, M.; Bertran, J.; Rodríguez-Santiago, L.; Baerends, E. J. *J. Phys. Chem. A* **1999**, *103*, 166–170. (c) Chermette, H.; Ciofini, I.; Mariotti, F.; Daul, C. *J. Chem. Phys.* **2001**, *115*, 11068–11079. (d) Grüning, M.; Gritsenko, O. V.; van Gisbergen, S. J. A.; Baerends, E. J.

J. Phys. Chem. A **2001**, 9211–9218. (e) Poater, J.; Solà, M.; Rimola, A.; Rodríguez-Santiago, L.; Sodupe, M. *J. Chem. Phys. A* **2004**, 6072–6078. (f) Metz, M.; Solomon, E. I. *J. Am. Chem. Soc.* **2001**, *123*, 4938–4950.

(52) (a) Cabrero, J.; Calzado, C. J.; Maynau, D.; Caballol, R.; Malrieu, J. P. *J. Phys. Chem. A* **2002**, *106*, 8146–8155. (b) Aebersold, M. A.; Guillon, B.; Plantevin, O.; Pardi, L.; Kahn, O.; Bergerat, P.; v. Seggern, I.; Tuczek, F.; Öhrström, L.; Grand, A.; Lelièvre-Berna, E. *J. Am. Chem. Soc.* **1998**, *120*, 5238–5245.

(53) Aboelella, N. W.; Kryatov, S. V.; Gherman, B. J.; Brennessel, W. W.; Young, V. G., Jr.; Sarangi, R.; Rybak-Akimova, E. V.; Hodgson, K. O.; Hedman, B.; Solomon, E. I.; Cramer, C. J.; Tolman, W. B. *J. Am. Chem. Soc.* **2004**, *126*, 16896–16911.

(54) Tyeklár, Z.; Jacobson, R. R.; Wei, N.; Murthy, N. N.; Zubieta, J.; Karlin, K. D. *J. Am. Chem. Soc.* **1993**, *115*, 2677–2689.

JP9040716